Hindawi Publishing Corporation
International Journal of Photoenergy
Volume 2007, Article ID 13653, 8 pages
doi:10.1155/2007/13653

Research Article

Photochemical Characterization and Photocatalytic Properties of a Nanostructure Composite TiO_2 Film

Mohammad Hossein Habibi,[1] Mojtaba Nasr Esfahani,[1] and Terry A. Egerton[2]

[1] *Department of Chemistry, University of Isfahan, Isfahan 81746-73441, Iran*
[2] *School of Chemical Engineering and Advanced Materials, University of Newcastle upon Tyne, Bedson Building, Newcastle NE1 7RU, UK*

Received 28 March 2006; Revised 11 July 2006; Accepted 9 October 2006

Recommended by Sabry Abdel-Mottalab

An efficient and new composite titania film photocatalyst was fabricated by sol-gel technique, using precalcined nanopowder titanium dioxide filler mixed with a sol, spin coating, and heat treatment. The structural and photocatalytic properties of these films were characterized using SEM, XRD, and UV/Vis spectroscopies. Problems of film inhomogenity and defects which caused peeling and cracking during calcination because of film shrinkage were overcome by using methylcellulose (MC) as a dispersant. Composite films heat-treated at approximately 500°C have the greatest hardness values. Surface morphology of composite deposits by scanning electron microscopy (SEM) showed that the composite films have much rougher surface than films made without MC. Photocatalytic activities of the composites film were evaluated through the degradation of three commercial diazo textile dyes, Light Yellow X6G (C.I. Reactive Yellow 2), Solophenyl red 3BL (C.I. Direct 80), and Tertrodirect light blue R (C.I. Direct blue 71) as a model pollutant.

1. INTRODUCTION

Industrial textile dyes are present in wastewaters at different concentrations. Dye pollutants in wastewaters are the principal source of environmental aqueous contamination. They need to be removed from wastewaters by different methods. Photocatalysis has been successfully used to oxidize many organic pollutants and particularly to decolorize dyes. Among the new oxidation methods or "advanced oxidation processes" (AOP), heterogeneous photocatalysis appears as an emerging destructive technology leading to the total mineralization of many organic pollutants. Some organic pollutants have been shown to be degraded and ultimately mineralized completely under UV irradiation on nanosized titania catalysts. Catalytic activity of titanium dioxide is based on the electron/hole pair formed upon photo excitation. A great deal of research has been conducted recently to optimize the performance of the TiO_2 photocatalysts with high surface area [1–7]. Composite materials can often be more efficient photocatalysts than pure substances. This phenomenon arises through the generation of new active sites due to interactions between titania and dopant oxides, through improved mechanical strength, thermal stability, and surface area of doped titania [8–10].

The use of slurries in wastewater treatment has some disadvantages: the separation of fine particles is slow and penetration of light is limited. These problems can be minimized by supporting TiO_2 on various materials. Many techniques have been developed to obtain advanced material based on TiO_2 [11–20]. Nanostructured materials are preferred over dense structures, because of their larger active surface. The production of nanostructured films is nowadays an established method and TiO_2 nanoparticles and mesoporous films are among the materials routinely produced through the sol-gel chemistry processing [21–25]. It is very important to prepare TiO_2 films that are capable of harvesting incident light to a great extent, and at the same time films with a high surface area and porosity to increase the rate of reaction between photogenrated species and the pollutants. Increasing the surface area of film is a promising way to improve the desired functions because almost all of these applications utilize the chemical reactions on the surface [26, 27]. Porous TiO_2 thin and thick films with large specific surface area have attracted more and more attention. The sol-gel process is generally

recognized to be an efficient route for fabricating homogeneous porous films by incorporating organic polymer with precursor solution [28, 29]. However these porous films are not thick enough to satisfy the need of practical applications.

To reach required thickness of the films, the sol-gel and dip or spin coating process is often repeated a number of times. Another way is to increase the viscosity of the precursor solution to increase the film thickness through a single dip or spin coating. However, the tensile stress induced by the shrinkage of the films during heat treatment may lead to peeling off or cracking of the films when the layer is thicker. Very low fraction of solid content (<10 vol%), suspended in the solvent, accounts for this high rate of dimensional change. However, the problem associated with the high rates of shrinkage can be overcome by the introduction of a secondary phase (e.g., precalcined powder, fibers, etc.) as a filler, to reinforce the resulting composite structure. Though this process, not only the high values of dimensional change from gel to dry body are reduced, but also the sol-gel derived material, present as a thin layer coating in between the precalcined particles, acts as a binder to bond the entire structure. The sol-gel derived material, present in between the neighboring particles, also acts as a sintering aid to decrease the sintering temperature. In some cases, this may result in densification of the composite at relatively low temperatures, as compared to the densification temperature of the same material prepared through conventional methods [30]. In this work we have increased the total surface area with the use of a TiO_2 with high surface area and the use of methylcellulose as a template and low-cost material.

In continuation of our ongoing programme to develop solid films for photocatalytic and photoelectrocatalytic purposes [31–33], herein, we report the photochemical characterization and photocatalytic activity of new nanostructure composite TiO_2 films prepared via sol-gel process and characterized using SEM, XRD measurements. We have evaluated the photocatalytic activities of the composites film using three commercial diazo textile dyes, Light Yellow X6G (C.I. Reactive Yellow 2), Solophenyl red 3BL (C.I. Direct 80), and Tertrodirect light blue R (C.I. Direct blue 71) as a model pollutant.

2. EXPERIMENTAL

2.1. Composite TiO_2 nanostructure preparation

Titanium tetraisopropoxide ($Ti(OPr)_4$ or TTP) (Aldrich, 97%), the precursor, was used without further purification. Anhydrous ethyl alcohol was used as the solvent to prevent fast hydrolysis of titanium alkoxide. Methylcellulose (Harris Chemical) was used to increase the viscosity of the sol and to better dispersion of TiO_2 nanopowder. TTP first was added to 10 ml ethanol and 1.8 ml HCl (35.5%) over five minutes while the solution was vigorously stirred for a further 120 minutes after the room temperature addition of the TTP. HCl catalyst was used to control the rate of condensation and to prevent fast gelation of the sol. In a separated container, methylcellulose solution (2 wt. % in double distilled deionized water was prepared. Then these two solutions (titania sol and MC solution) were mixed and stirred overnight for around 2 hours at room temperature. TiO_2, anatase nanopowder (Aldrich), stated to have a surface area of ∼190–290 m^2/gr and a particle size ∼15 nm (5 wt.%), was used as filler that mixed the sol to prepare the composite nanostructure film. TiO_2 nanopowder was ultrasonically dispersed into the final sol. The stability of the suspension is controlled by altering the TiO_2 nanopowder and MC concentration. The prepared mixture was deposited on the microscope glass slides (7.5 mm × 2.5 mm × 1 mm) by a homemade spin coater (∼2000 rpm). The coated samples were dried at room temperature for 1 day, and then heat treated at 100°C and 500°C for 1 hours.

2.2. Catalyst characterization

Microstructures of the prepared samples, after being coated with gold, were observed by scanning electron microscopy (SEM) Philips XL30, operated at 20 kV, and working distance of minimum 4 mm for the highest magnification. The phase composition of photocatalyst was studied by plate XRD technique. The X-ray diffraction patterns were obtained on a D8 Advanced Bruker X-ray diffractometer using Cu Kα radiation at an angle of 2θ from 15° to 60°. The scan speed was 0.03 $2\theta \cdot S^{-1}$. The strongest peaks of TiO_2 corresponding to anatase (1 0 1) were selected to evaluate the crystallinity of the samples. The mean crystallite size L was determined from the broadening β of the most intense line, for each polymorph, in the X-ray diffraction pattern, based on the Scherer equation

$$L = \frac{k\lambda}{\beta \cos\theta}, \tag{1}$$

where λ is the radiation wavelength, $k = 0.90$, and θ is the Bragg angle [34].

Evaluation of the adhesion and bonding strength between the coating and substrate has been made by using the scratch test technique [35]. The mechanical integrity of coatings (deposited by spin coating method with the same controlled thickness) was measured using a Motorised Clemen scratch tester (equipped with a tungsten carbide ball tool 1 mm). Scratches were made under an applied load increasing from 0 to 1000 g, for the maximum length of 50 mm. The point of coating adhesive failure was determined by visual observation. The load at which the indenter started to scratch the substrate surface was considered as indicative of the coating resistance to scratch failure.

2.3. Photocatalytic activity tests

The photocatalytic activity of the nanostructure TiO_2 films was evaluated by the degradation of three diazo dyes. Light Yellow X6G dye (C.I. Reactive Yellow 2, M.W. = 872.5 gr/mol), Solophenyl red 3BL (C.I. Direct 80, M.W. = 1373 g/mol), and Tertrodirect light blue R (C.I. Direct blue 71, M.W. = 783 gr/mol) textile dyes were obtained from Bitterfeld (Germany), Ciba-Geigy (UK), and Crompton & Knowles

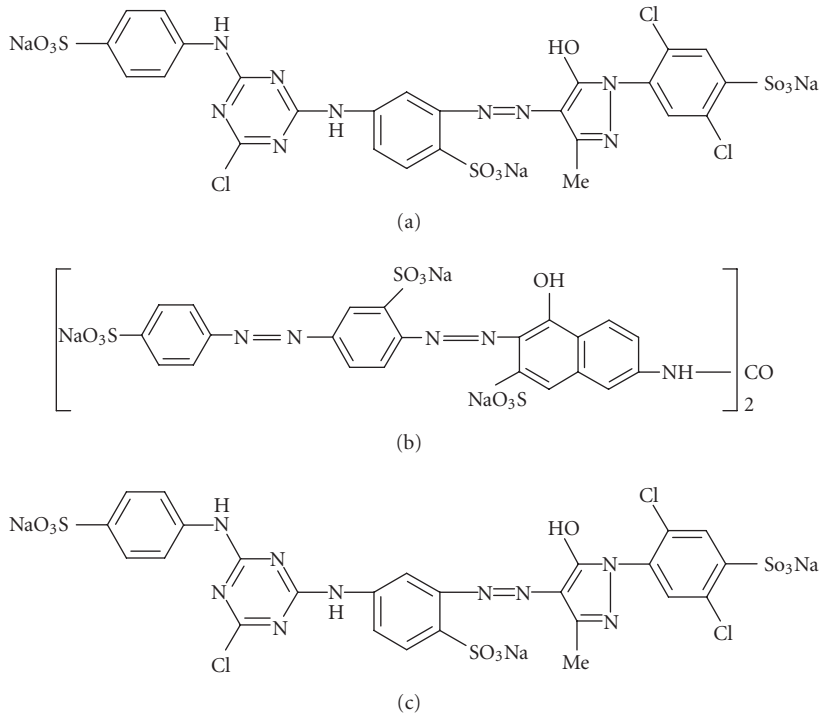

Figure 1: (a) Chemical structure of commercial diazo dye of Light Yellow X6G (C.I. Reactive Yellow 2). (b) Chemical structure of commercial diazo dye of Solophenyl red 3BL (C.I. Direct 80). (c) Chemical structure of commercial diazo dye of Tertrodirect light blue R (C.I. Direct blue 71).

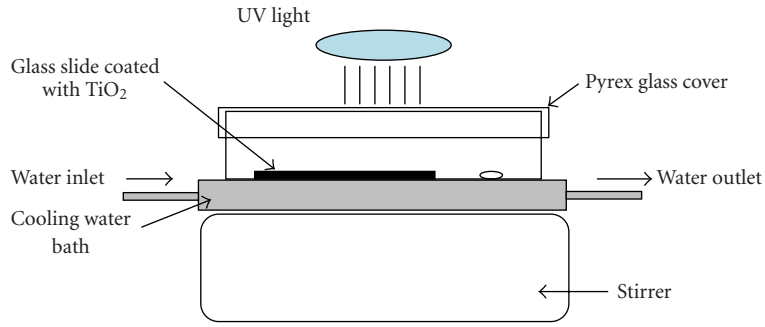

Figure 2: Schematic diagram of photoreactor for degradation of diazo dyes.

Corp. (USA), respectively, as typical pollutants in the textile industry. Dye chemical structures are shown in Figures 1(a)–1(c).

All photocatalytic activity experiments were carried out using a simple (40 cm ×15 cm ×15 cm) oxidation reactor placed in a 25°C water bath (Figure 2).

A singly coated slide was irradiated with two 8W UVA (Philips, $\lambda = 365$ nm) lamps placed 5 cm above the solution. Aqueous solutions of (10 ml) of each dye solution with initial pH 6.0 and initial concentration of 10 ppm were stirred continuously and samples were taken at regular interval during irradiation and analyzed by a double beam UV–visible spectrophotometer (Varian Cary 500 Scan) to monitor photocatalytic degradation of X6G, 3BL, and Tertrodirect light blue R at 400, 530, and 570 nm, respectively. For comparison, the contaminants solution was also photolyzed in the absence of photocatalyst to examine their stability. In that case, the experimental results verify that the azo dyes are not decomposed even after long-time irradiation. To evaluate the catalytic strength changes due to immobilization of the TiO_2 nanopowder and compare the films (with and without MC) efficiency to the TiO_2 nanopowder, the film weight was measured. The slurry concentration of TiO_2 was then adjusted to meet the exact quantity of TiO_2 nanopowder immobilized film (160 ppm), in order to safely compare the obtained results.

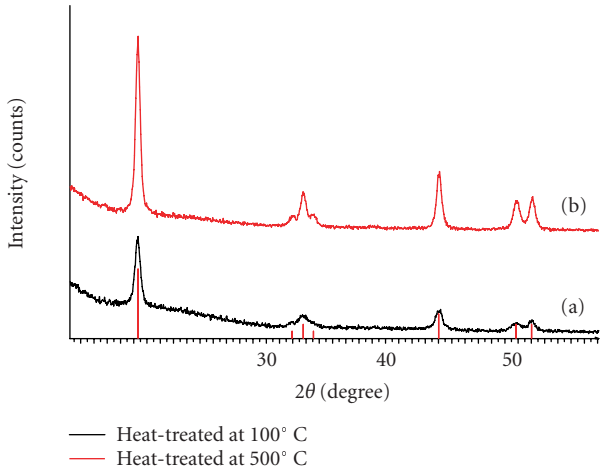

Figure 3: XRD patterns for TiO_2 composite film with MC: (a) heat treated at 100°C and (b) heat treated at 500°C.

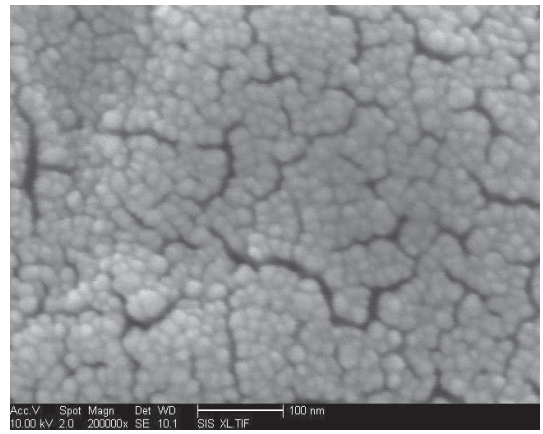

Figure 4: SEM images of the composite nanostructure TiO_2 film with MC after heat treatment at 500°C.

3. RESULTS AND DISCUSSION

3.1. XRD and SEM characterization of nanostructure composite TiO_2 film

Different compositions of TiO_2 sol prepared by altering the molar ratio of TTP : H_2O : HCl. MC addition increased the sedimentation time of 5% powder dispersions from 1 to 70 hours and of the 10% powder from 0.5 to 10 hours. Although the increased viscosity of the MC addition fluid will lower sedimentation rates, the decreased sedimentation rate is believed to be associated primarily with the better dispersion of the nanopowders that results from their steric stabilization by MC.

The X-ray diffractograms of the composites prepared from anatase nanopowder dispersed in the alkoxide sols after heat treatment are shown in Figure 3. All peaks (2θ = 25.28, 37.02, 37.80, 38.82, 48.05, 53.9, and 55.06) correspond to known diffraction maxima of anatase. By calcination in 500°C, the (101) peak of anatase has become sharper, which indicates the dependence of crystallinity on the applied temperature.

The average crystallite size of TiO_2 was calculated by Scherrer's equation using the full width at half maximum (FWHM) of the X-ray diffraction peaks at $2\theta = 25.28°$ for anatase. Typical values of anatase crystallite size of the synthesized TiO_2 particles on glass were 16.5 ± 0.5 nm. Similar sizes were measured for the filler powder and for the composite films, with or without MC. Therefore, the size of the TiO_2 crystallites, derived from the sol, does not affect the size of final crystallites (shown in Table 1). The SEM image of the surface of composite TiO_2 film heat treated at 500°C for 60 minutes (Figure 4) demonstrates the nanostructure of composite film and shows particle size of TiO_2 in SEM image corresponding to XRD results.

The annealing process at 500°C resulted in stronger bond to the substrate according to the mechanical test results shown in Table 1. The resulting coating has porous microstructure (Figure 4), and therefore is resistant to cracking during drying and heat treatment.

3.2. Photodegradation of various diazo dyes

A preliminary test was done to obtain a few sets of standard control data for each dye used in the photodegradation experiments. The preliminary test was carried out in the dark using the prepared photocatalyst. The results reported in Table 2 confirmed that the removal of dyes was insignificant for the mentioned condition. It must be stressed that total removal of the diazo dyes was not contributed by the effect of photodegradation alone. A small portion of the removal efficiency was attributable to the rapid attainment of adsorption equilibrium of the dyes onto TiO_2 composite film/glass with Tertro direct light blue R being the most significant (6.8%). However, when the photodegradation experiments were carried out under illumination of light, total removal of pollutant was enhanced significantly. Total removal of pollutant can be attributed to more than 90% of photodegradation capability in addition to the above-mentioned surface adsorption effect.

Optimum set of parameter was used for each of the experiment to investigate the effectiveness of photodegradation process using glass loaded composite TiO_2 on various types of diazo dye. Removal efficiency of different types of dye is reported in Figure 5. It shows that the concentration of each type of dye decreased effectively with time.

To illustrate diazo dyes disappearance and intermediate products, we present UV visible spectrum of all three dyes in Figures 5, 6, and 7. It is known that the color of azo dyes such as X6G and others is determined by the azo bonds (N=N) and their associated chromophores and auxochromes [36]. The absorption peaks, corresponding to the color of X6G, 3BL, and Tertrodirect light blue R at λ_{max} = 400, 530, and 567 nm, respectively, and another, corresponding to Π to Π* transition of aromatic rings of dyes at 270 nm, were

Table 1: Physical and chemical characteristics of composite TiO_2 film, compared to TiO_2 nanopowder.

Material	Heat treatment conditions	Scratch adhesion (g/mm^2)[a]	Particle size (nm)
TiO_2 nanopowder	—	~ 0	15.2
	500°C	~ 0	16.3
Composite thick film with sol without MC	—	7	15.3
	500°C	150	16.4
Composite thick film with sol and MC	—	9	15.2
	500°C	200	16.3

[a]Critical linearly increasing loads.

Table 2: Preliminary test and experiments carried out applying optimum parameters. One piece of composite TiO_2 film, two pieces of blue fluorescent lamp, 10 mL of each dye solution with initial pH 6.0 and initial concentration of 10 ppm, and temperature (25°C) with illumination time 300 minutes.

	Initial concentration (ppm)	Adsorption removal[a] (ppm/%)	Photodegradation removal[b] (ppm/%)	Total removal[c] (ppm/%)
Light Yellow X6G	10.45	0.051/0.5	9.945/95.2	9.996/95.7
Solophenyl red 3BL	10.33	0.072/0.7	9.679/93.7	9.751/94.4
Tertrodirect blue R	10.25	0.697/6.8	9.009/87.9	9.706/94.7

[a]Total removal in the dark using photocatalyst.
[b]Total removal-adsorption removal = photodegradation removal.
[c]Total removal under light illumination using photocatalyst applying optimum parameters.

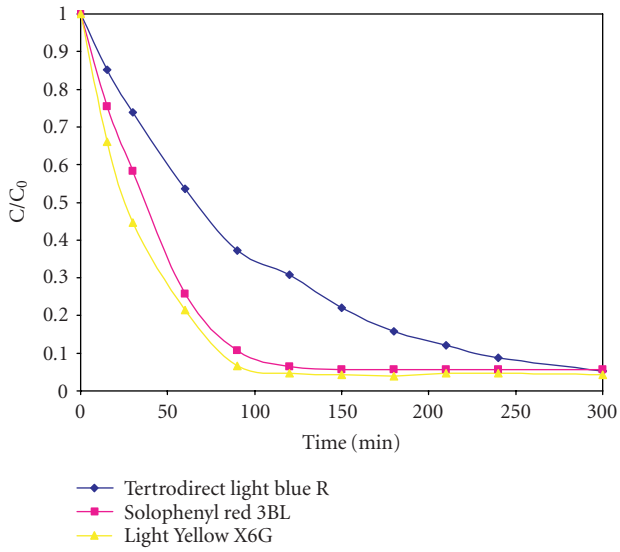

Figure 5: Graph C/C_0 versus time, t (min) for the removal efficiency of different types of dyes. One piece of composite TiO_2 with MC/glass, two pieces of blue fluorescent lamp, 10 mL of each dye solution with initial pH 6.0, initial concentration of 10 ppm, and temperature (28°C).

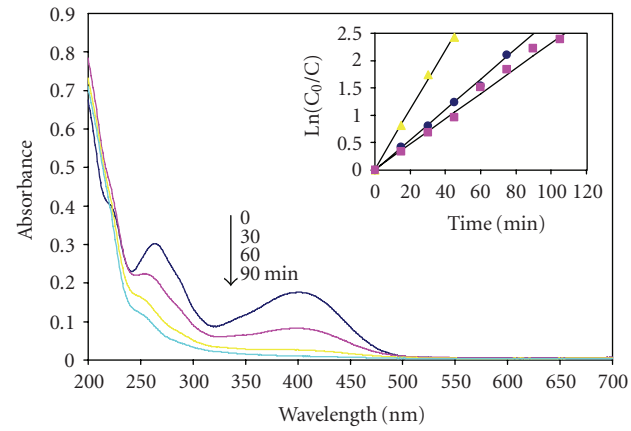

Figure 6: Time-dependent UV-Vis spectrum of X6G solution during photoirradation on one piece of composite TiO_2 with MC, pH 6.00, dye concentration, 10 ppm. The inset of the figure shows the kinetic data for this dye in the presence of slurry nanopowder TiO_2 (160 ppm) solution (▲) composite thick film without MC (■), and composite thick film with MC (•).

diminished and finally disappeared under reaction which indicated that the dyes had been degraded. No new absorption bands appear in the visible or ultraviolet regions. As indicated by the absorbance at 400, 530, and 567 nm, the X6G, 3BL, and Tertrodirect light blue R, respectively, were decolorized faster than disappearance of the absorbance at 270 nm. These results indicate that the fast decolorized dyes were followed by much slower mineralization of intermediates formed subsequently.

UV irradiation of all of the TiO_2 materials slurries, composite film with or without MC resulted in an effective photocatalytic decomposition of the three azo dyes. To a first

Table 3: Pseudo-first-order kinetic parameters of three diazo dyes photocatalytic degradation .

Dye	Composite film with MC		Composite film without MC		Suspension of TiO_2 nanopowder (160 ppm)	
	$K_{app} \times 10^{-2}$ (min^{-1})	$t_{1/2}$ (min)	$K_{app} \times 10^{-2}$ (min^{-1})	$t_{1/2}$ (min)	$K_{app} \times 10^{-2}$ (min^{-1})	$t_{1/2}$ (min)
Light Yellow X6G	2.77	25	2.31	30	5.47	12.7
Solophenyl red 3BL	1.80	38.5	0.77	90	5.38	12.9
Tertrodirect blue R	1.01	68.6	0.50	138.6	5.26	13.2

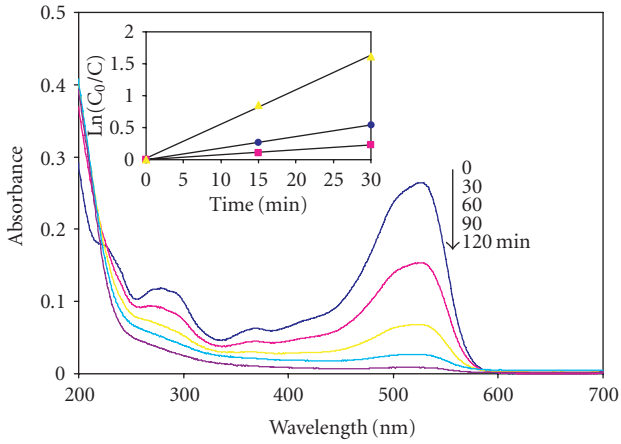

Figure 7: Time-dependent UV-Vis spectrum of 3BL solution during photoirradation on one piece of composite TiO_2 with MC, pH 6.00, dye concentration, 10 ppm. The inset of the figure shows the kinetic data for this dye in the presence of slurry nanopowder TiO_2 (160 ppm) solution (▲) composite thick film without MC (■), and composite thick film with MC (•).

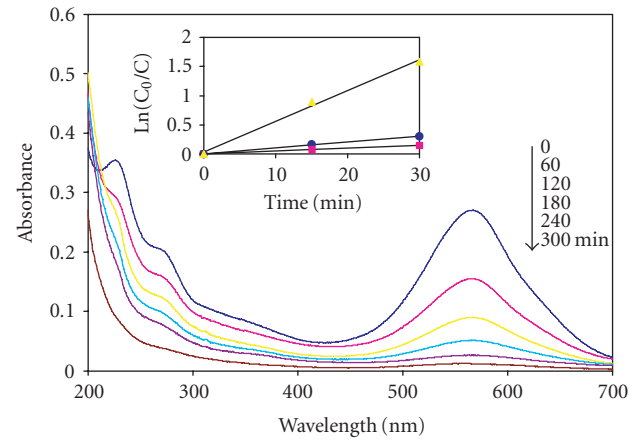

Figure 8: Time-dependent UV-Vis spectrum of Tertro direct light blue solution during photoirradation on one piece of composite TiO_2 with MC, pH 6.00, dye concentration, 10 ppm. The inset of the figure shows the kinetic data for this dye in the presence of slurry nanopowder TiO_2 (160 ppm) solution (▲), composite thick film without MC (■), and composite thick film with MC (•).

approximation, the three modes of degradation (i.e., slurry TiO_2 and two composite films with and without MC) seem to follow first-order reaction kinetics, that is, plots of $\ln(C_0/C)$ versus time in the optimized conditions were linear (the insets of Figures 5, 6, and 7). This is consistent with, but does not prove, the generally held view that photodegradation rates of chemical compounds on semiconductor surfaces follow the Langmuir-Hinshelwood model [37]. The pseudo-first-order reaction rate constants and half-life parameters are listed in Table 3. The results show that photodegradation process using composite titanium dioxide supported on glass is most effective in removing all three dyes. As higher removal efficiency will have a higher apparent rate constant, k_{app} value, shorter time was needed for the dye to be totally photodegraded as confirmed by the half-time, $t_{1/2}$ value in Table 3. It is shown that the half-time needed to photodegrade X6G is just 25 minutes. It is suggested that photodegradation efficiency of each dye may be affected by their molecular size. A bigger molecular size of the dye may require prolong experimental time for it to be photodegraded completely. Since the molecular size of 3BL is much bigger than the X6G as shown in Figures 1(a) and 1(b) (X6G = 872.5 g/mol, 3BL = 1373 g/mol) lower removal efficiency of it seems to be acceptable. However, Tertro direct light blue with molecular weight 783 g/mol has a smaller molecular size but it has lowest photodegradation efficiency. It can be explained that this dye is absorbed more strongly and irreversibly on the surface of composite film (as shown in Table 3) and blocked the active sites on the surface of composite film to saturation and lower rates of degradation on composite film. It was further noticed that this dye has four SO_3Na groups with three naphthalene rings to help it to absorb strongly on composite film.

To compare the photocatalytic degradation of composite TiO_2 film with nanopowder slurry, the dye solution (10 ml) was also photolyzed in the presence of a suspension (dispersion) of TiO_2 nanopowder with the same weight of film (0.0016 g = 160 ppm) and the results are represented in the insets of Figures 5, 6, and 7 (▲). The rate constant for the slurry is greater than that of the two films, suggesting a considerably higher efficiency as photocatalyst. This may be due to limitations of reactant diffusion or it may be because only the external surface of the film samples is exposed to the pollutant solution and therefore the effective area is much less than the (190–290 m^2/g) of the TiO_2 nanopowder.

All of the insets of Figures 6, 7, and 8 (■ and •) demonstrate that the rate constant for the composite film with MC is greater than that of the film without MC. It is possible that

the increased activity of the MC additioned film for photodegradation of these three azo dyes is due to its greater porosity, nanostructure (as is seen in Figure 4) and that the higher photoefficiency is due to the greater accessible surface area. The results as plotted seem to be in the reverse order. Even if the rates are greater for MC film, the difference is really significant.

4. CONCLUSION

It is evident that the photocatalytic degradation of various diazo dyes illuminated by UVA fluorescent lamp gives a promising result in the presence of nanostructure TiO_2 composite coated on glass plates. This new composite titania film photocatalysts were fabricated by sol-gel technique, using precalcined nanopowder titanium dioxide filler mixed with a sol and heat treatment by spin coating. The structural and photocatalytic properties of these films were characterized using SEM, XRD, and UV/Vis spectroscopies. Composite films with MC as dispersant heat treated at approximately 500°C have the greatest hardness values. Surface morphology of composite deposits by scanning electron microscopy (SEM) showed that the composite films have much rougher surface than films made without methylcellulose. Photocatalytic activities of the composites film were evaluated through the degradation of a textile dye, Light Yellow X6G (C.I. Reactive Yellow 2) as a model pollutant.

Therefore, although surface active site TiO_2 decreases with immobilization (coating on a substrate) with using nanopowder TiO_2 with high surface area, we can almost modify this reduction in surface area of a TiO_2 film.

ACKNOWLEDGMENTS

The authors wish to thank the University of Isfahan for supporting this work financially. Authors wish to thank Kermanshah Oil Refinery for their partial support.

REFERENCES

[1] M. R. Hoffmann, S. T. Martin, W. Choi, and D. W. Bahnemann, "Environmental applications of semiconductor photocatalysis," *Chemical Reviews*, vol. 95, no. 1, pp. 69–96, 1995.

[2] U. Siemon, D. W. Bahnemann, J. J. Testa, D. Rodríguez, M. I. Litter, and N. Bruno, "Heterogeneous photocatalytic reactions comparing TiO_2 and Pt/TiO_2," *Journal of Photochemistry and Photobiology A: Chemistry*, vol. 148, no. 1–3, pp. 247–255, 2002.

[3] T. López, R. Gómez, E. Sanchez, F. Tzompantzi, and L. Vera, "Photocatalytic activity in the 2,4-dinitroaniline decomposition over TiO_2 sol-gel derived catalysts," *Journal of Sol-Gel Science and Technology*, vol. 22, no. 1-2, pp. 99–107, 2001.

[4] P. C. A. Alberius, K. L. Frindell, R. C. Hayward, E. J. Kramer, G. D. Stucky, and B. F. Chmelka, "General predictive syntheses of cubic, hexagonal, and lamellar silica and titania mesostructured thin films," *Chemistry of Materials*, vol. 14, no. 8, pp. 3284–3294, 2002.

[5] E. L. Crepaldi, G. J. de A. A. Soler-Illia, D. Grosso, F. Cagnol, F. Ribot, and C. Sanchez, "Controlled formation of highly organized mesoporous titania thin films: from mesostructured hybrids to mesoporous nanoanatase TiO_2," *Journal of the American Chemical Society*, vol. 125, no. 32, pp. 9770–9786, 2003.

[6] R. Vogel, P. Meredith, I. Kartini, et al., "Mesostructured dye-doped titanium dioxide for micro-optoelectronic applications," *Chemistry and Physical Chemistry*, vol. 4, no. 6, pp. 595–603, 2003.

[7] J. C. Yu, J. Yu, and J. Zhao, "Enhanced photocatalytic activity of mesoporous and ordinary TiO_2 thin films by sulfuric acid treatment," *Applied Catalysis B: Environmental*, vol. 36, no. 1, pp. 31–43, 2002.

[8] M. E. Zorn, D. T. Tompkins, W. A. Zeltner, and M. A. Anderson, "Catalytic and photocatalytic oxidation of ethylene on titania-based thin-films," *Environmental Science & Technology*, vol. 34, no. 24, pp. 5206–5210, 2000.

[9] J. Kim, K. C. Song, S. Foncillas, and S. E. Pratsinis, "Dopants for synthesis of stable bimodally porous titania," *Journal of the European Ceramic Society*, vol. 21, no. 16, pp. 2863–2872, 2001.

[10] M. E. Manríquez, T. López, R. Gómez, and J. Navarrete, "Preparation of TiO_2-ZrO_2 mixed oxides with controlled acid-basic properties," *Journal of Molecular Catalysis A: Chemical*, vol. 220, no. 2, pp. 229–237, 2004.

[11] N. Serpone and E. Pelizzetti, Eds., *Photocatalysis. Fundamentals and Applications*, Wiley Interscience, New York, NY, USA, 1989.

[12] H. A. Al-Ekabi and D. Ollis, Eds., *Photocatalytic Purification and Treatment of Water and Air*, Elsevier Science B. V., Amsterdam, The Netherlands, 1993.

[13] D. W. Bahnemann, J. Cunningham, M. A. Fox, E. Pelizzetti, P. Pichat, and N. Serpone, "Photocatalytic treatment of waters," in *Aquatic Surface and Photochemistry*, R. G. Zepp, G. R. Helz, and D. G. Crosby, Eds., pp. 261–316, Lewis, Boca Raton, Fla, USA, 1994.

[14] M. Schiavello, Ed., *Photocatalysis and Environment. Trends and Applications*, Kluwer Academic, Dordrecht, The Netherlands, 1988.

[15] J.-M. Herrmann, "Water treatment by heterogeneous photocatalysis," in *Environmental Catalysis*, F. Jansen and R. A. van Santen, Eds., vol. 1 of *Catalytic Science Series*, pp. 171–194, Imperial College Press, London, UK, 1999.

[16] A. Houas, H. Lachheb, M. Ksibi, E. Elaloui, C. Guillard, and J.-M. Herrmann, "Photocatalytic degradation pathway of methylene blue in water," *Applied Catalysis B: Environmental*, vol. 31, no. 2, pp. 145–157, 2001.

[17] M. Vautier, C. Guillard, and J.-M. Herrmann, "Photocatalytic degradation of dyes in water: case study of indigo and of indigo carmine," *Journal of Catalysis*, vol. 201, no. 1, pp. 46–59, 2001.

[18] C. Guillard, J. Disdier, C. Monnet, et al., "Solar efficiency of a new deposited titania photocatalyst: chlorophenol, pesticides and dyes removal applications," *Applied Catalysis B: Environmental*, vol. 46, no. 2, pp. 319–332, 2003.

[19] M. Karkmaz, E. Puzenat, C. Guillard, and J.-M. Herrmann, "Photocatalytic degradation of the alimentary azo dye amaranth - mineralization of the azo group to nitrogen," *Applied Catalysis B: Environmental*, vol. 51, no. 3, pp. 183–194, 2004.

[20] K. R. Gopidas and P. V. Kamat, "Photochemistry on surfaces. 4. Influence of support material on the photochemistry of an adsorbed dye," *Journal of Physical Chemistry*, vol. 93, no. 17, pp. 6428–6433, 1989.

[21] C. Guillard, B. Beaugiraud, C. Dutriez, et al., "Physicochemical properties and photocatalytic activities of TiO_2-films prepared by sol-gel methods," *Applied Catalysis B: Environmental*, vol. 39, no. 4, pp. 331–342, 2002.

[22] C. H. Kwon, H. Shin, J. H. Kim, W. S. Choi, and K. H. Yoon, "Degradation of methylene blue via photocatalysis of titanium dioxide," *Materials Chemistry and Physics*, vol. 86, no. 1, pp. 78–82, 2004.

[23] J. Yu and X. Zhao, "Effect of surface treatment on the photocatalytic activity and hydrophilic property of the sol-gel derived TiO_2 thin films," *Materials Research Bulletin*, vol. 36, no. 1-2, pp. 97–107, 2001.

[24] J. C. Yu, H. Y. Tang, J. Yu, et al., "Bactericidal and photocatalytic activities of TiO_2 thin films prepared by sol-gel and reverse micelle methods," *Journal of Photochemistry and Photobiology A: Chemistry*, vol. 153, no. 1–3, pp. 211–219, 2002.

[25] Y. U. Ahn, E. J. Kim, H. T. Kim, and S. H. Hahn, "Variation of structural and optical properties of sol-gel TiO_2 thin films with catalyst concentration and calcination temperature," *Materials Letters*, vol. 57, no. 30, pp. 4660–4666, 2003.

[26] K. Kajihara and T. H. Yao, "Sol-gel derived macroporous titania films prepared from the system containing poly(ethylene glycol) together with long-chain alcohols," *Journal of Sol-Gel Science and Technology*, vol. 17, no. 3, pp. 239–245, 2000.

[27] M. M. Yosuf, H. Imai, and H. Hirashima, "Preparation of mesoporous TiO_2 thin films by surfactant templating," *Journal of Non-Crystalline Solids*, vol. 285, no. 1–3, pp. 90–95, 2001.

[28] K. Kajihara, K. Nakanishi, K. Tanaka, K. Hirao, and N. Soga, "Preparation of macroporous titania films by a sol-gel dip-coating method from the system containing poly(ethylene glycol)," *Journal of the American Ceramic Society*, vol. 81, no. 10, pp. 2670–2746, 1998.

[29] S. J. Bu, Z. G. Jin, X. X. Liu, H. Y. Du, and Z. J. Cheng, "Preparation and formation mechanism of porous TiO_2 films using PEG and alcohol solvent as double-templates," *Journal of Sol-Gel Science and Technology*, vol. 30, no. 3, pp. 239–248, 2004.

[30] D. E. Clark, "Sol-gel derived ceramic matrix composites," in *Science of Ceramic Chemical Processing*, L. L. Hench and D. R. Urlich, Eds., John Wiley & Sons, New York, NY, USA, 1986.

[31] M. H. Habibi and N. Talebian, to appear in *Dyes Pig*.

[32] M. H. Habibi and N. Talebian, "The effect of annealing on structural, optical and electrical properties of nanostructured tin doped indium oxide thin films," *Acta Chimica Slovenica*, vol. 52, no. 1, pp. 53–59, 2005.

[33] A. Hassanzadeh, M. H. Habibi, and A Zeini Isfahani, "Study of electronic structure of tin-doped In_2O_3 (ITO) film deposited on glass," *Acta Chimica Slovenica*, vol. 51, no. 3, pp. 507–527, 2004.

[34] R. A. Spurr and H. Myers, "Quantitative analysis of anatase-rutile mixtures with an X-ray diffractometer," *Analytical Chemistry*, vol. 29, no. 5, pp. 760–762, 1957.

[35] M. Keshmiri, T. Mohseni, and T. Troczynski, "Development of novel TiO_2 solgel-derived composite and its photocatalytic activities for trichloroethylene oxidation," *Applied Catalysis B: Environmental*, vol. 53, no. 4, pp. 209–219, 2004.

[36] C. Zhu, L. Wang, L. Kong, et al., "Photocatalytic degradation of azo dyes by supported TiO_2 + UV in aqueous solution," *Chemosphere*, vol. 41, no. 3, pp. 303–309, 2000.

[37] A. Houas, H. Lachheb, M. Ksibi, E. Elaloui, C. Guillard, and J.-M. Hermann, "Photocatalytic degradation pathway of methylene blue in water," *Applied Catalysis B: Environmental*, vol. 31, no. 2, pp. 145–157, 2001.